Thickness-Dependent Transmission in a Finite Photonic Crystal Containing Nearly Ferroelectric Superconductor

Heng-Tung Hsu, *Senior Member, IEEE*, and Chien-Jang Wu, *Member, IEEE*

***Abstract*—In this paper, anomalous transmission properties in a finite photonic crystal made of a nearly ferroelectric superconductor, and a dielectric have been theoretically investigated. We show that, in the thickness domain, the transmission spectrum can be divided into two different regions: nonresonance and resonance. There are resonant transmission peaks in the resonance region, and the number of peaks is strongly dependent on the number of periods. In the frequency response, the number of resonant peaks is also increased as the thickness of nearly ferroelectric superconductor increases. The appearance of anomalous peaks enables us to design a narrowband filter without introducing any defect layer into the photonic crystal.**

***Index Terms*—Photonic crystal, transmission, nearly ferroelectric superconductor, narrowband filter.**

I. Introduction

PHOTONIC crystals (PCs), artificially periodic structures made of media with refractive indices, have attracted much attention over the last two more decades [1]. Depending on the spatial arrangement, PCs can be classified as 1-D, 2-D, and 3-D, respectively. Due to the periodic feature in structure, there can exist certain forbidden regions in the photonic band structure (PBS) for a PC. These regions are called photonic band gaps (PBGs) which are analogous to the electronic band gaps in solids. The existence of PBGs enables us to design the PC as a reflector which is, indeed, of particular use in modern semiconductor laser systems.

The PBS as well as PBG are strongly dependent on the constituents in PCs. Recently, PCs containing superconducting materials called superconducting photonic crystals (SPCs) have been of great interest to the communities of optics and condensed matter physics [2]–[17]. It is shown that, in an SPC, there is a low-frequency cutoff frequency, which is not seen in an all-dielectric PC [2], [5], [16], [17]. The use of superconducting thin film can control the properties of defect modes in a defective SPC [11], [12]. Moreover, SPC containing magnetic films has been experimentally shown to have a negative refractive index, an important consequence of double-negative materials [6].

The aforementioned reports of SPC almost concentrate on typical high-temperature cuprate, $YBa_2cu_30_{7x}$ (YBCO) or conventional superconducting system, Niobium (Nb). In addition to these two familiar superconductors, there exists a special kind of superconductor called the nearly ferroelectric (NFE) superconductors. An NFE superconductor is not only in the superconducting state but in NFE state. An NFE state indicates that the material is a soft-mode ionic system with a fairly high static permittivity. There have been two systems that belong to the NFE superconductors. The first is the Na-doped WO_3, i.e., sodium tungsten bronze Na_xWO_3 with $x \sim 0.05$. It is a high-temperature superconductor with critical temperature $T_c \sim 90$ K [18]. The second is the n- or p-doped $SrTiO_3$ (STO) with a relatively low transition temperature, $T_c \sim 1 - 3$ K [19], [20]. The host STO is a NFE material with a very high static permittivity, $\varepsilon(0) \sim 10^4$ when it is in the superconducting state [21].

Research on the SPCs containing NFE superconductor is rarely seen thus far. The purpose of this paper is thus to explore the electromagnetic wave transmission properties in a finite SPC made of an NFE superconductor and a dielectric. The NFE superconductor will be considered to operate in the dielectric-like region. This is an anomalous region because its permittivity function is positive, sharply contrary to the usual superconductors whose permittivity function is negative. We will investigate the effect of thickness of NFE superconductor on the transmission in such SPC structure.

The format of this work is described as follows: In Section II, we first briefly review the electrodynamics of an NFE superconductor. Then, matrix method is given to calculate the transmission spectrum. In Section III, we present the numerical results and discussion. Finally, the concluding remarks are given in Section IV.

II. Basic Equations

Let us consider a finite binary SPC denoted as $(AB)^N$, where layer A is the NFE superconductor, layer B is the dielectric, and N is the number of periods. The thicknesses of A and B are d_a and d_b, respectively. In addition, their corresponding refractive indices are n_a and n_b, respectively. The SPC is assumed to be immersed in air. For an NFE superconductor, the index of refraction is related to the wave number $k_{\rm NFE}$, namely

$$n_a = \frac{c}{\omega} k_{\rm NFE} \quad (1)$$

Manuscript received June 1, 2014; revised August 15, 2014; accepted August 17, 2014. This work was supported by the National Science Council of the Republic of China (Taiwan) under Grant NSC-100-2112-M-003-005-MY3.

H.-T. Hsu is with the Department of Communication Engineering, Yuan Ze University, Chungli 320, Taiwan (e-mail: htbeckhsu@saturn.yzu.edu.tw).

C.-J. Wu is with the Institute of Electro-Optical Science and Technology, National Taiwan Normal University, Taipei 11677, Taiwan (e-mail: jasperwu@ntnu.edu.tw).

Color versions of one or more of the figures in this paper are available online at http://ieeexplore.ieee.org.

Digital Object Identifier 10.1109/JSTQE.2014.2350012

where c is the velocity of light, ω is the circular frequency, and where $k_{\rm NFE}$ can be obtained from the wave equation, which is expressed as

$$\nabla^2\mathbf{E}+\left(\omega^2\mu_0\varepsilon(\omega)-\frac{\mu_0}{\Lambda}\right)\mathbf{E}=0 \qquad (2)$$

based on the electrodynamics of NFE superconductors [22]. That is

$$k_{\rm NFE}=\left[\omega^2\mu_0\varepsilon(\omega)-\frac{\mu_0}{\Lambda}\right]^{1/2} \qquad (3)$$

In Eq. (2), μ_0 is the permeability of free space, $\mathbf{E}$ is the electric field, and the permittivity function $\varepsilon(\omega)$ comes from the ionic lattice vibration given by [23]

$$\varepsilon(\omega)=\varepsilon'_\infty\frac{\omega_{LO}^2-\omega^2}{\omega_{TO}^2-\omega^2} \qquad (4)$$

where $\omega_{\rm LO}$ and $\omega_{\rm TO}$ are the longitudinal and transverse soft-mode lattice frequencies, respectively, and

$$\varepsilon'_\infty=\varepsilon_\infty\Pi'_i\omega_{Li}^2/\omega_{Ti}^2 \qquad (5)$$

where the primed product over i includes all oscillations except the soft mode and additionally the frequency w is assumed to be well below all ω_{Ti} and ω_{Li}. In addition, the parameter Λ is Eq. (2) is written by

$$\Lambda=\frac{m*}{N_se^2}=\mu_0\lambda_L^2 \qquad (6)$$

where N_s is the concentration of super-electrons, m^* is the electron effective mass, and e is the electronic charge, and λ_L is known as the London penetration length. It can be seen from Eq. (3) that if $k_{\rm NFE}$ is imaginary, then the wave will damp with a frequency-dependent penetration depth λ_L^* given by

$$\lambda_L^*=\frac{\lambda_L}{\sqrt{1-\omega^2\mu_0\varepsilon(\omega)\lambda_L^2}}. \qquad (7)$$

This is the familiar Meissner response of a superconductor. On the other hand, if k is real, then electromagnetic waves will propagate in the NFE superconductor, just like in a dielectric material. In this case, we have the dielectric-like response or the anomalous response for an NFE superconductor. In the analysis that follows, we shall pay our attention to this dielectric-like response in the study of transmission properties for the NFE SPC.

To calculate the transmittance for the considered SPC of $(AB)^N$, matrix formulation will be employed. According to 2×2 matrix method, the amplitudes of reflected wave E_{ro} and transmitted wave E_{to} must be determined in terms of incident wave E_{io}. The result is given by [24]

$$\begin{aligned}E_{t0}\begin{bmatrix}1\\ \eta_0^{-1}\end{bmatrix}&=M_{\rm cell}^N\begin{bmatrix}E_{i0}+E_{r0}\\ \eta_0^{-1}(E_{i0}-E_{r0})\end{bmatrix}\\&=M_{\rm system}\begin{bmatrix}E_{i0}+E_{r0}\\ \eta_0^{-1}(E_{i0}-E_{r0})\end{bmatrix}\\&=\begin{bmatrix}m_{11}&m_{12}\\ m_{21}&m_{22}\end{bmatrix}\begin{bmatrix}E_{i0}+E_{r0}\\ \eta_0^{-1}(E_{i0}-E_{r0})\end{bmatrix} \qquad (8)\end{aligned}$$

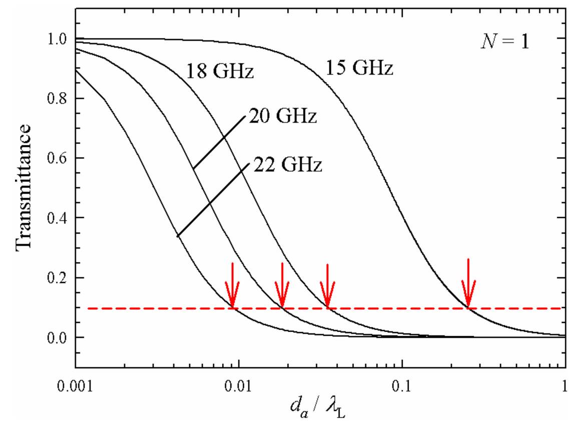

Fig. 1. Transmittance versus thickness of NFE layer d_a for a single period ($N=1$) at 15 GHz and $d_b=\lambda_L/4$, where $\lambda_L=18\ \mu$m.

where η_0 is the wave impedance of free space and

$$M_{\rm cell}=\exp\left\{i\omega d_b\begin{bmatrix}0&\mu_0\\ \varepsilon_0\varepsilon_b&0\end{bmatrix}\right\}\exp\left\{i\omega d_a\begin{bmatrix}0&\mu_0\\ \varepsilon_0\varepsilon_a&0\end{bmatrix}\right\}. \qquad (9)$$

Here, ε_b is the permittivity of dielectric layer. Then the reflection coefficient Γ and transmission coefficient τ can be obtained to be

$$\Gamma=\frac{m_{11}\eta_0+m_{12}-\eta_0^2m_{21}-m_{22}\eta_0}{-m_{11}\eta_0+m_{12}+\eta_0^2m_{21}-m_{22}\eta_0} \qquad (10)$$

$$\tau=m_{11}(1+\Gamma)+\frac{m_{12}}{\eta_0}(1-\Gamma). \qquad (11)$$

The transmittance is thus given by $\tau^*\tau$.

III. Numerical Results and Discussion

In this paper, in our numerical calculations, we shall consider n-STO as our NFE superconductor because its material parameters are available. They are $\omega_{\rm TO}=1.6\times10^{11}$ rad/s, $\omega_{\rm LO}=5.2\times10^{12}$ rad/s, $\varepsilon_\infty=5.5\varepsilon_0$, $\Pi'_i\omega_{Li}^2/\omega_{Ti}^2=4.1$, $m^*=10m_0$, and $N_s=9\times10^{17}$ cm^{-3} [22]. With these parameters, the calculated London penetration length is $\lambda_L=18\mu$m and the dielectric-like response can be obtained to be in the frequency range of $\omega_{c1}(=0.9\times10^{11}\text{rad/s})-\omega_{\rm TO}$. In the linear frequency, it is $f=14.3-25.4$ GHz, which is the frequency range of interest in this work. The dielectric layer is $LaAlO_3$ with a permittivity of $\varepsilon_b=24$ [25], [26].

In Fig. 1, we first plot the transmittance versus the thickness of NFE layer d_a for a single period, $N=1$ and $d_b/\lambda_L=1/4$. It can be seen that transmittance in the thickness domain is a decreasing function of d_a at a fixed frequency. That is, high transmission is obtainable at d_a well below the penetration length λ_L. At 15 GHz there will be zero transmission when d_a approaches or is larger than λ_L. Zero transmission means a total reflection, which is a common result in a superconducting material. The results in Fig. 1 reflects the skin size effect which arises from the thickness of NFE layer. By the way, the curves are similar to those of low-pass filters in the usual frequency domain [27]. Thus, we can define the threshold thickness (indicated by the

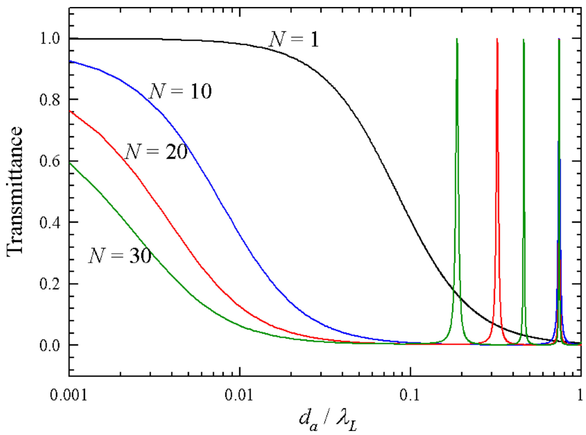

Fig. 2. Transmittance versus thickness of NFE layer d_a for distinct periods, $N = 1$, 10, 20, and 30, respectively, at 15 GHz and $d_b = \lambda_L/4$, where $\lambda_L = 18\ \mu$m.

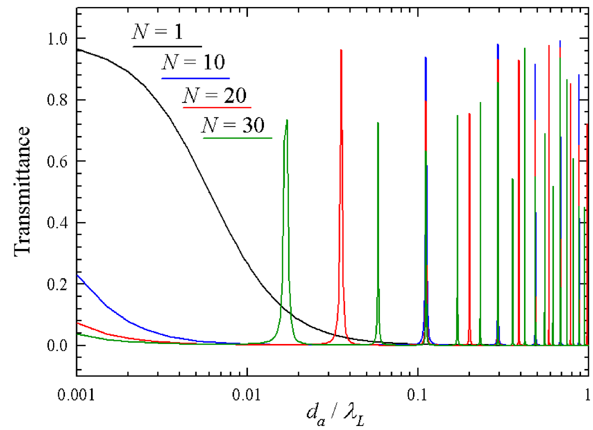

Fig. 4. Transmittance versus thickness of NFE layer d_a for distinct periods, $N = 1$, 10, 20, and 30, respectively, at 20 GHz and $d_b = \lambda_L/4$, where $\lambda_L = 18\ \mu$m.

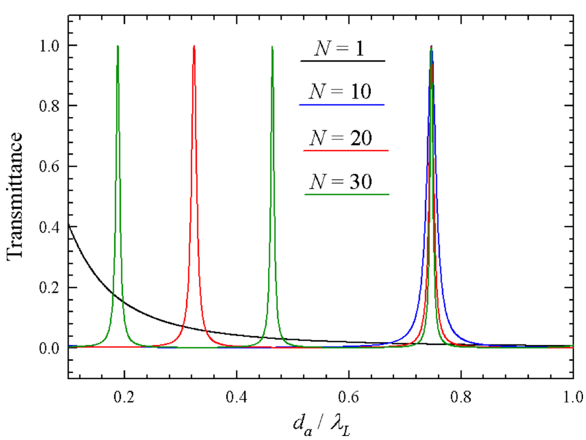

Fig. 3. A re-plot of Fig. 2 for the range of $d_a/\lambda_L = 0.1 - 1.0$.

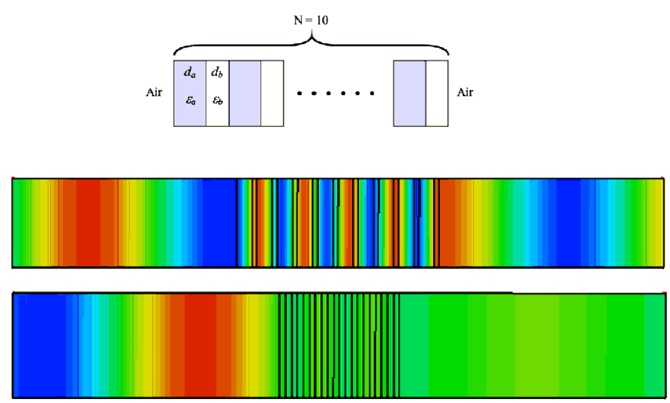

Fig. 5. The spatial distribution of the calculated E-field at 15 GHz when $d_a = 0.75\lambda_L$ (upper) and $d_a = 0.5\lambda_L$ (lower), corresponding to the occurrence of peak-transmittance and zero-transmittance, respectively. In both cases, the thickness of the $LaAlO_3$ is fixed to be $\lambda_L/4$.

red arrow) at which the magnitude of transmittance equals 0.1, then we can find that the threshold thickness will decrease as the frequency increases.

Next, we examine the effect of number of periods on the transmittance. By taking frequency at 15 GHz, transmittance curves are plotted in Fig. 2, where different $N = 1$, 10, 20, and 30 are taken, respectively. As the number of periods increases, the transmittance curves are quite different from that of $N = 1$. The low-pass behavior in Fig. 1 is heavily suppressed and in the meantime anomalous transmission peaks are created. More importantly, it is of interest to note that the transmittance is divided into two regions. One is for nonresonance (like in Fig. 1) occurring in the region of $d_a/\lambda_L < 0.1$, where transmittance is decreased as *N* increases. The other is the resonant region when $d_a/\lambda_L > 0.1$. In this region, the number of the resonant peaks will be increased as *N* increases. A detailed look at the resonant part is shown in Fig. 3. For different *N*'s, there exists a common peak in the vicinity of $d_a/\lambda_L = 0.75$. If we now increase the frequency to 20 GHz, results of transmittance are depicted in Fig. 4. In this case, many peaks are produced at a large value of *N*.

The behaviors of resonance and nonresonance can be clearly elucidated by the study the field intensity versus thickness. To do so, we have performed numerical simulation using a commercial simulator (CST Studio Suite 2014) which is based on the finite integration in time domain algorithm. Based on the curve of Fig. 2 for the case $N = 10$, Fig. 5 shows the spatial distribution of the calculated E-field intensity profile at 15 GHz when $d_a = 0.75\lambda_L$, corresponding to the occurrence of peak-transmittance (resonance). Another case for $d_a = 0.5\lambda_L$, corresponding to the occurrence of zero-transmittance (nonresonance), is also included in the same plot. In both cases, the thickness of the $LaAlO_3$ is fixed to be $\lambda_L/4$. The difference in the intensity for the two cases is obvious as shown. For the case when peak-transmittance occurs, significant field intensity can be obtained within and throughout the periodic structure. On the contrary, however, none of the incident field can penetrate into the structure when zero-transmittance occurs.

Next, we study the frequency response of the transmittance. In Fig. 6, we plot the transmittance at different number of periods, $N = 1$, 6, 10, and 20, respectively. Here,

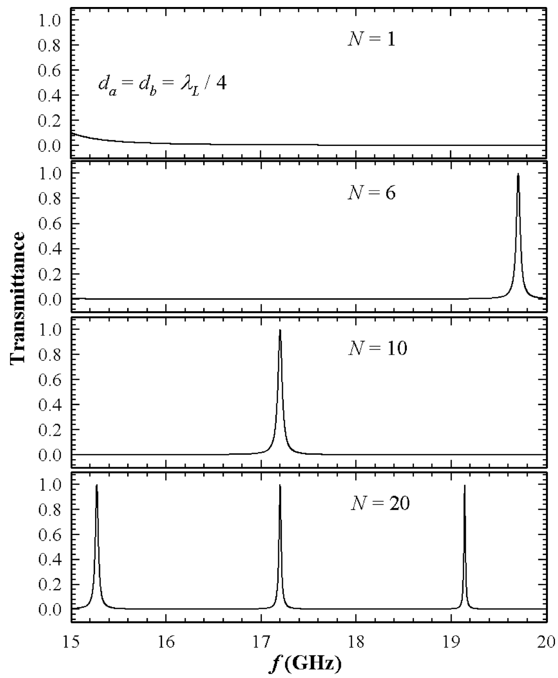

Fig. 6. Frequency response of transmittance at distinct periods, $N = 1, 6, 10$, and 20, respectively, at $d_a = d_b = \lambda_L/4$, where $\lambda_L = 18$ μm.

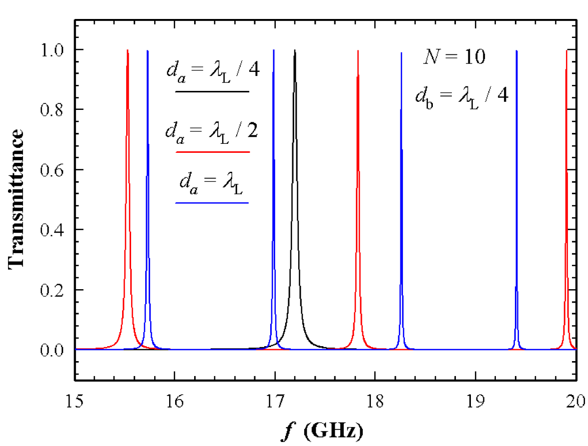

Fig. 7. Frequency response of transmittance at $N = 10$ and $d_b = \lambda_L/4$ for three different $d_a = \lambda_L/4, \lambda_L/2$, and λ_L, respectively.

$d_a/\lambda_L = d_b/\lambda_L = 1/4$ is taken. Some features are of note. First, we have found that the first resonant peak starts to show up when N is equal or greater than six. Second, the peak is then red-shifted as N increases. Finally, multiple peaks will be present at a large number of periods, say $N = 20$. The results illustrate that the presence of anomalous transmission peaks is strongly dependent on the number of periods of the SPC. Taking $N = 10$, the effect of thickness is depicted in Fig. 7, in which we fixed the dielectric layer at $d_b/\lambda_L = 1/4$ and change d_a/λ_L to $1/4$, 1/2, and 1, respectively. It can be seen that more peaks will be produced as d_a increases.

IV. Summary

We have studied the thickness-dependent anomalous transmission properties in a finite SPC containing NFE superconductor. We have shown that there can be total transmission in such SPC when the NFE superconductor is operated in the dielectric-like region. The number of transmission peaks can be increased as the number of periods increases. It can also be increased as the thickness of NFE layer increases. The increase in the peak numbers can be ascribed as follows. In the resonance where peak occurs, the whole structure can be regarded as an effective Airy slab [28]. It is known that the peak number will be increased as the width of slab increases. In addition, it is worth mentioning that, to best of our knowledge, there has been no experimental works related to the current considered structure thus far, partly because the NFE superconductor is a very special class of superconductor. Thus, this work may provide a motivation to the experimental works to study electromagnetic wave properties in a layered structure containing NFE superconductors. Finally, the appearance of resonant transmission peaks make it possible in designing the multiple-channel filter based on the use of SPC without having any defect layer.

References

[1] J. D. Jannopoulos, S. G. Johnson, J. N. Winn, and R. D. Meade, *Photonic Crystals: Molding the Flow of Light*, 2nd ed. Princeton, NJ, USA: Princeton Univ. Press, 2008.

[2] C. H. Raymond Ooi, T. C. Au Yeung, C. H. Kam, and T. K. Lim, “Photonic band gap in a superconductor-dielectric superlattice,” *Phys. Rev. B*, vol. 61, pp. 5920–5923, 2000.

[3] H. Takeda and K. Yoshino, “Tunable photonic band schemes in two dimensional photonic crystals composed of copper oxide high temperature superconductors,” *Phys. Rev. B*, vol. 67, pp. 245109-1–245109-4, 2003.

[4] H. Takeda and K. Yoshino, “Properties of Abrikosov lattices as photonic crystals,” *Phys. Rev. B*, vol. 70, pp. 085109-1–085109-5, 2004.

[5] C.-J. Wu, M.-S. Chen, and T.-J. Yang, “Photonic band structure for a superconductor-dielectric superlattice,” *Physica C*, vol. 432, pp. 133–139, 2005.

[6] A. Pimenov, A. Loidl, P. Przyslupski, and B. Dabrowski, “Negative refraction in Ferromagnet-superconductor superlattices,” *Phys. Rev. Lett.*, vol. 95, pp. 247704-1–247704-4, 2005.

[7] O. L. Berman, Y. E. Lozovik, S. L. Eiderman, and R. D. Coalson, “Superconducting photonic crystals: Numerical calculations of the band structure,” *Phys. Rev. B*, vol. 74, pp. 092505-1–092505-3, 2006.

[8] T. H. Pei and Y. T. Huang, “A temperature modulation photonic crystal Mach–Zehnder interferometer composed of copper oxide high-temperature superconductor,” *J. Appl. Phys.*, vol. 101, pp. 084502-1–084502-5, 2007.

[9] H. Rauh and Y. A. Genenko, “The effect of a superconducting surface layer on the optical properties of a dielectric photonic composite,” *J. Phys., Condens. Matter*, vol. 20, pp. 145203-1–145203-4, 2008.

[10] A. N. Poddubny, E. L. Ivchenko, and Yu. E. Lozovik, “Low-frequency spectroscopy of superconducting photonic crystals,” *Solid State Commun.*, vol. 146, pp. 143–147, 2008.

[11] I. L. Lyubchanskii, N. N. Dadoenkova, A. E. Zabolotin, Y. P. Lee, and T. Rasing, “A one-dimensional photonic crystal with a superconducting defect layer,” *J. Opt. A, Pure Appl. Opt.*, vol. 11, pp. 114014-1–114014-4, 2009.

[12] N. N. Dadoenkova, A. E. Zabolotin, I. L. Lyubchanskii Y. P. Lee, and T. Rasing, “One-dimensional photonic crystal with a complex defect containing an ultrathin superconducting sublayer,” *J. Appl. Phys.*, vol. 108, pp. 093117-1–093117-4, 2010.

[13] W.-H. Lin, C.-J. Wu, T.-J. Yang, and S.-J. Chang, “Terahertz multichanneled filter in a superconducting photonic crystal,” *Opt. Exp.*, vol. 18, pp. 27155–27166, 2010.

[14] S. M. Anlage, “The physics and applications of superconducting metamaterials,” *J. Opt.*, vol. 13, pp. 024001-1–024001-5, 2011.

[15] Yu. S. Dadoenkova, N. N. Dadoenkova, I. L. Lyubchanskii Y. P. Lee, and T. Rasing, "Effect of lateral shift of the light transmitted through a one-dimensional superconducting photonic crystal," *Photon. Nanostruc.-Fundamentals Appl.*, vol. 11, pp. 345–352, 2013.
[16] C. A. Hu, C.-J. Wu, T.-J. Yang, and S.-L. Yang, "Analysis of effective plasma frequency in a superconducting photonic crystal," *J. Opt. Soc. Amer. B*, vol. 30, pp. 366–369, 2013.
[17] J.-J. Wu and J.-X. Gao, "Ultra-wide low-frequency band gap of one-dimensional superconducting photonic crystals containing metamaterials," *J. Supercond. Novel. Magn.*, vol. 27, pp. 667–672, 2014.
[18] Y. Levi, O. Millo, A. Sharoni, Y. Tsabba, G. Leitus, and S. Reich, "Evidence for localized high-Tc superconducting regimes on the surface Na-doped WO3," *Europhys. Lett.*, vol. 51, pp. 564–570, 2000.
[19] M. L. Cohen, "Superconductivity in many-valley semiconductors and in semimetals," *Phys. Rev.*, vol. 134, pp. A511–A521, 1964.
[20] C. S. Konnce, M. L. Cohen, J. E. Schooley, W. R. Hosler, and L. F. Pfeiffer, "Superconducting transition temperature of semiconducting SrTiO3," *Phys. Rev. B*, vol. 163, pp. 380–390, 1967.
[21] E. Savaguchi, A. Kukuchi, and Y. Codera, "Dielectric constant of strontium titanate at low temperature," *J. Phys. Soc. Jpn.*, vol. 17, pp. 1666–1667, 1962.
[22] J. L. Birman and N. A. Zimbovskaya, "Electrodynamics of nearly ferroelectric superconductors," *Phys. Rev. B*, vol. 64, pp. 144506-1–144506-8, 2001.
[23] M. Born and K. Huang, *Dynamical Theory of Crystal Lattices*. New York, NY, USA: Oxford Univ. Press, 1954.
[24] A. Lakhtakia, "Linear optical responses of nematic thin films (SNTFs)," *Optik*, vol. 106, pp. 45–52, 1997.
[25] C. M. Nelson, M. Spies, L. S. Abdallah, S. Zollner, Y. Xu, and H. Luo, "Dielectric function of LaAlO3 from 0.8 to 6 eV between 77 and 700 K," *J. Vac. Sci. Technol. A*, vol. 30, pp. 061404-1–061404-6, 2012.
[26] P. Hartemann, "Effective and intrinsic surface impedances of high-*T*c superconducting thin films," *IEEE Trans. Appl. Supercond.*, vol. 2, no. 4, pp. 228–235, Dec. 1992.
[27] R. C. Dorf and J. A. Svoboda, *Introduction to Electric Circuits*. New York, NY, USA: Wiley, 2004.
[28] P. Yeh, *Optical Waves in Layered Media*. Singapore: Wiley, 1991.

Heng-Tung Hsu (S'98–M'03–SM'05) received the B.S. and M.S. degrees in electronics engineering from the National Chiao Tung University, Hsinchu, Taiwan, in 1993 and 1995, respectively, and the Ph.D. degree in electrical and computer engineering from the University of Maryland, College Park, MD, USA, in 2002.

He joined Yuan Ze University (YZU), Jhongli, Taiwan, in 2005, where he is currently an Associate Professor with the Department of Communication Engineering. His research interests include electromagnetic theory and wave propagation, antenna design, active and passive microwave components, and RF packaging.

Dr. Hsu received the Young Scholar Research Award at YZU in 2011 and the Y. Z. Hsu Outstanding Professor Award in 2012.

Chien-Jang Wu (M'01) was born in Yunlin, Taiwan, on March 1, 1962. He received the B.S. degree in electronics engineering, the M.S. degree in electrooptical engineering, and the Ph.D. degree in solid-state electronics from National Chiao Tung University (NCTU), Hsinchu, Taiwan, in 1985, 1990, and 1996, respectively.

He was a Liquid-Crystal-Display Design Engineer, Seiko Epson, Taipei, Taiwan, from 1990 to 1991. He was also a Telecommunication Hardware Engineer with TranSystem, Inc., Hsinchu from 1991 to 1992. He was also an Electromagnetic Compatibility, Electromagnetic Interference, and Telecommunication Certification Engineer with the Electronic Test Center, Taipei in 1992. In 1993, he began to work toward the doctoral degree at NCTU, where his research was mainly in the theory of microwave superconductivity and vortex dynamics. He later was briefly associated with the Department of Physics, National Sun Yat-sen University, Kaohsiung, Taiwan, before joining National Formosa University, Yunlin, Taiwan, in August 1997, where he was an Assistant Professor from 1997 to 2000, an Associate Professor from 2000 to 2003, and a Full Professor from 2003 to 2005. In February 2005, he joined the Department of Applied Physics, National University of Kaohsiung, Kaohsiung, Taiwan, where he was the Chair from 2006 to 2008. In February 2008, he joined the Institute of Electrooptical Science and Technology, National Taiwan Normal University, Taipei, where he is currently a Full Professor and was the Director of Institute from August 2008 to July 2011. He was invited as a Consultant Researcher in the Solid-State Electronics Laboratory, Department of Physics, National Tsinghua University from July to October 2001. His current research interests include electromagnetic/microwave theory, theory of microwave superconductivity with vortex dynamics, and calculation of optical properties of materials, including metamaterials, superconductors, graphenes, and photonic bandgap crystals.

Dr. Wu has been a Fellow of the Electromagnetics Academy since 2007. He is a Member of the Optical Society of America. He became a Member of the IEEE Microwave Theory and Techniques Society and Photonics Society.